Environmental Science
Processes & Impacts

Oxalate-Enhanced Solubility of Lead (Pb) in the Presence of Phosphate: pH Control on Mineral Precipitation

Journal:	*Environmental Science: Processes & Impacts*
Manuscript ID	EM-ART-11-2018-000553.R1
Article Type:	Paper
Date Submitted by the Author:	13-Mar-2019
Complete List of Authors:	McBride, Murray; Cornell University, Crop and Soil Sciences Kelch, Sabrina; Cornell University, Biological and Environmental Engineering Schmidt, Michael; Cornell University, Soil and Crop Sciences Sherpa, Sonam ; Cornell University College of Arts and Sciences, School of Integrative Plant Sciences Martinez, Carmen Enid; Cornell University, Soil and Crop Sciences Section Aristilde, Ludmilla; Cornell University, Biological and Environmental Engineering

Oxalate-Enhanced Solubility of Lead (Pb) in the Presence of Phosphate: pH Control on Mineral Precipitation

Authors: Murray B. McBride,[A,]* Sabrina E. Kelch,[A] Michael P. Schmidt,[A] Sonam Sherpa, [A]

Carmen Enid Martinez,[A] and Ludmilla Aristilde[B]

Affiliations: [A]*Soil and Crop Sciences Section, School of Integrative Plant Science, College of Agriculture and Life Sciences, Cornell University, Ithaca, USA*

[B]*Department of Biological and Environmental Engineering, College of Agriculture and Life Sciences, Cornell University, Ithaca, NY, USA*

** Corresponding author (e-mail* mbm7@cornell.edu*)*

Abstract

Here we study the precipitation of lead (Pb)-phosphate minerals over the pH range of 4.0 to 8.0 with and without oxalate, a ubiquitous and abundant low-molecular-weight organic acid derived from plants and microorganisms in environmental matrices. In the aqueous Pb-phosphate systems, phosphate precipitated Pb efficiently, reducing the dissolved Pb concentration below 1 μM at all the tested pH values, with the minimum solubility of about 0.1 μM measured at the intermediate pH of 6.0. The measured dissolved Pb and free Pb^{2+} ion activity were not in agreement with predictions from generally-accepted solubility products of the Pb phosphate minerals, particularly hydroxypyromorphite $[Pb_5(PO_4)_3OH]$. Discrepancies between our measured Pb phosphate solubility products and older reported values are attributed to non-ideal behavior of these minerals (incongruent dissolution) as well as uncertainties in stability constants for soluble Pb-phosphate ion pairs. The presence of equimolar levels of oxalate and phosphate resulted in up to 250-fold increase in Pb solubility at acidic pH and about a 4-fold increase at pH 7.0, due to the strong suppression of Pb phosphate precipitation by oxalate and formation of soluble Pb-oxalate complexes. At pH 4.0 and 5.0, Fourier transform infrared spectroscopy (FTIR) and X-ray diffraction (XRD) identified a Pb-oxalate mineral phase as the only precipitate despite the presence of phosphate; in the absence of oxalate, Pb hydrogen phosphate, $PbHPO_4$, stably formed under these acidic conditions. At pH 6.0 and greater, FTIR and XRD data revealed that Pb-phosphate $[Pb_3(PO_4)_2]$, and hydroxypyromorphite $[Pb_5(PO_4)_3OH]$ to a lesser extent, were the predominant precipitates both in the absence and presence of oxalate. Therefore, oxalate did not strongly interfere with Pb-phosphate mineral formation at aqueous pH greater than 6.0 but oxalate controlled Pb solubility at acidic pH values.

Environmental Significance

The precipitation of low-solubility Pb minerals, including Pb-phosphates, can limit Pb bioavailability and mobility in contaminated soils. However, the formation of these minerals can be impaired by the presence of low-molecular-weight organic acids. Here, we investigated the inhibition of Pb-phosphate precipitation by oxalate. We uncovered marked discrepancies between our data and predicted Pb solubility based on older reported Pb mineral solubility products widely used in chemical speciation models. We combined a wet chemical approach with spectroscopic and X-ray diffraction data examinations to investigate the potential impact of oxalate on Pb phosphate mineral formation and solubility. In summary, Pb phosphate solid phases were stable in the presence of oxalate at pH 6.0 or higher, but Pb-oxalate was the prevalent solid phase at pH 5 or less.

Introduction

Human health risk from soils contaminated with lead (Pb), a toxic heavy metal, is primarily assessed based on the total Pb concentration in soils.[1] However, the bioavailability of toxic metals including Pb depends on metal solubility and lability, which can vary greatly in soils.[2,3] Using isotopic exchangeability, labile Pb has been found to vary between 7% and 99% of total soil Pb depending on the source of Pb contamination and soil properties.[4] One of the most promising methods of stabilizing Pb in soils and reducing its solubility and bioavailability is the use of phosphate amendments to form insoluble Pb-phosphate precipitates.[5] However, in soils, bioweathering of Pb phosphates by metabolic exudates from plants and microorganisms can alter Pb lability.[6] Specifically, the secretion of low-molecular-weight organic acids including oxalate can play a prominent role in controlling Pb solubility.[7-9] Previous studies have reported that these organic acids and other dissolved organic matter in soil solutions enhanced Pb solubility by promoting dissolution of pyromorphite and other Pb-phosphate minerals.[7, 10-14] Oxalate-induced Pb dissolution in the rhizosphere of plants growing in high-Pb growth media was shown to result in enhanced uptake of Pb into the plant tissues.[9] Beyond facilitating the dissolution of existing minerals, oxalate secreted by fungal colonies has been shown to transform pyromorphite into crystalline Pb oxalate, a mineral that can be more stable than Pb-phosphate minerals in the acidic pH range.[6]

In this study, we investigated the chemical processes constraining Pb immobilization as Pb-phosphates in the absence and presence of oxalate, a ubiquitous organic acid in plant and microbial secretions. The relevant chemical equations and widely used reaction equilibrium constants for the precipitation of Pb by phosphate complexation are the following for the formation, respectively, of hydroxypyromorphite [$Pb_5(PO_4)_3OH$], Pb-phosphate [$Pb_3(PO_4)_2$], and Pb-hydrogen phosphate ($PbHPO_4$):

$$5Pb^{2+}{}_{(aq)} + 3H_2PO_4{}^{-}{}_{(aq)} + H_2O_{(l)} = Pb_5(PO_4)_3OH_{(s)} + 7H^{+}{}_{(aq)} \qquad \log K = 4.14 \qquad (1)$$

$$3Pb^{2+}{}_{(aq)} + 2H_2PO_4{}^{-}{}_{(aq)} = Pb_3(PO_4)_{2(s)} + 4H^{+}{}_{(aq)} \qquad \log K = 4.43 \qquad (2)$$

$$Pb^{2+}{}_{(aq)} + H_2PO_4{}^{-}{}_{(aq)} = PbHPO_{4(s)} + H^{+}{}_{(aq)} \qquad \log K = 4.35 \qquad (3)$$

These mineral formation constants, which are derived from the original research of Nriagu[15,16], appear in a number of computer programs such as Visual MINTEQ[17] used to calculate speciation of metal ions in water. The above equations are written with the phosphate species $H_2PO_4{}^{-}$ because it is predominant in the environmentally relevant pH range of 3 to 7. For the precipitation of Pb by oxalate to form the Pb-oxalate mineral (PbC_2O_4), the relevant chemical equation is:

$$Pb^{2+}{}_{(aq)} + C_2O_4{}^{2-}{}_{(aq)} = PbC_2O_{4(s)} \qquad \log K = 8.94 \qquad (4)$$

There is substantial disagreement in the published literature regarding the formation constants of Pb phosphates, particularly those of pyromorphites, the apatite-group minerals considered most likely to limit Pb availability in phosphate-amended soils. For example, the solubility product of chloropyromorphite, $Pb_5(PO_4)_3Cl$, has been repeatedly reported to be several orders of magnitude greater than the value published in earlier compilations of mineral solubility products and employed previously in chemical speciation calculations.[12,18-20] Kinetics may have some role in the reported inconsistencies in solubility as Henry et al.[5] stated that $Pb_5(PO_4)_3OH$ may age in soils to become more stable over time. However, Scheckel and Ryan[21] found that aging of $Pb_5(PO_4)_3Cl$ prepared in the laboratory ceased after one-day equilibration time; dissolution kinetics of the one-year aged mineral showed no difference from the one-day aged mineral. In addition to uncertainties regarding the thermodynamic stability of Pb phosphates, recent research[22] has reported a measured log formation constant of 11.13 for PbC_2O_4, which is substantially higher than older constants commonly used, such as the 8.94 value in the Visual MINTEQ database.[17a] The higher formation constant (lower solubility product) indicates that the Pb oxalate solid phase may be stable over a wider range of conditions in soil and water than previously assumed.

In the present study, we seek to evaluate two main hypotheses: (i) oxalate will interfere with Pb-phosphate mineral formation under conditions where both the oxalate and phosphate ligands are present at comparable concentrations in solution; (ii) Pb will be mobilized from insoluble Pb phosphate minerals by environmentally realistic concentrations of soluble oxalate. We conducted laboratory experiments to explore Pb solubility in aqueous solutions containing only phosphate, only oxalate, and both oxalate and phosphate over a wide range of pH (4.0 to 8.0). We combined this wet chemical approach with structural characterization of the corresponding precipitates by Fourier Transform Infrared (FTIR) spectroscopy, and X-ray diffraction (XRD). Our findings provide important insights towards predicting and evaluating the extent of Pb mobility and bioavailability in soils enriched in organic acid exudates from plants and microorganisms.

Experimental Methods

Pb-phosphate systems: preparation and chemical analysis

Stock solutions of 100 mM $Pb(NO_3)_2$ and 660 mM Na_2HPO_4 were prepared in deionized water and subsequently pre-adjusted to pH 4.0 with concentrated nitric acid (HNO_3) using a double-junction combination Orion pH glass electrode to measure pH. Measured volumes of these solutions were used to prepare (in three replicates) 100-mL volumes of aqueous solutions of 10 mM Pb^{2+} combined with 66 mM phosphate. In all scenarios, the Pb nitrate solution was added last after pre-adjustment of the phosphate solutions to pH 5.0, 6.0, 7.0 and 8.0 using concentrated NaOH in order to avoid initial formation of Pb hydroxide precipitates. The prepared solutions with visible suspended precipitates were then gently agitated at 22^{o}C for 10 days, after which the pH was measured to determine the effect of chemical reactions in shifting the solution pH. Thereafter, the solution pH was re-adjusted to the initial pH values (pH 4.0, 5.0, 6.0, 7.0, or 8.0). The suspensions were subsequently equilibrated for 24 hours before using 0.2 µm nitrocellulose membrane filtration to separate the solution phases from precipitated Pb mineral particles. The separated solutions were acidified with ultrapure nitric acid to a final concentration of 1.0 M HNO_3 prior to analysis of total dissolved Pb by inductively coupled plasma atomic emission spectrometry (ICP-AES). The Spectro Arcos ICP instrument was used in axial view mode, with the 220 nm atomic emission line of Pb selected for analysis because of its lack of spectral interferences and very good measured detection limit of 0.004 mg L^{-1}. Certified Pb standards and solution blanks in matched matrices of nitric acid were used to calibrate the instrument in the Pb concentration range of the sample solutions.

Solutions of Pb with phosphate (10 mM Pb^{2+}, 66 mM phosphate) were again prepared in triplicate as described above, but these solutions with their suspended mineral precipitates were allowed to age for an additional 7 months after the initial 10 day equilibration time. This time, in addition to the final pH values, the free Pb^{2+} ion activities of the suspensions were measured using a solid-state ion-selective Pb^{2+} electrode (YSI) with internal reference. The Pb electrode was calibrated by measuring millivolt response in 10^{-4} M $Pb(NO_3)_2$ solutions containing concentrations of Na oxalate between 0 and 0.01 M and buffered at pH 5.0 with 0.01 M Na acetate. The activities of free Pb^{2+} ions in these Pb activity buffer solutions were calculated using the chemical speciation program Visual Minteq[17] , and a calibration curve of log (Pb^{2+}) vs. millivolt reading was obtained over the log activity range of -4 to -8 . Repeat calibrations of the electrode over this activity range were conducted to test reproducibility of the measurements, and showed an average standard deviation of 0.9 mV or an error in the pPb values of about 0.03 units. None of the ionic species known to strongly interfere with the Pb^{2+} electrode measurements (e.g., Cu^{2+}, Ag^{+}, Cd^{2+}) were present in the solutions studied here.

Following the activity measurements, the 7 month-aged suspensions were filtered and the separated solutions were acidified using nitric acid. Dissolved aqueous Pb concentrations were determined by ICP-AES as described above.

Exposure of Pb phosphates to low oxalate concentration

To simulate the more realistic condition of both low dissolved phosphate and oxalate as would be expected in soil or water media, Pb phosphate solids precipitated from solution at pH 4, 6 and 8 after equilibration for 7 months (as described in the section above) were separated from the solutions onto Whatman #42 filter papers, then washed free of excess salts by repeated rinses with deionized water. After these solids were air-dried, duplicate 50 mg samples were placed into 50 ml plastic tubes and 20 ml of 10^{-3} M Na acetate buffer (pH 5.0) was added to each tube. A second set of duplicate Pb phosphate samples was identically prepared with the additional step of adding 0.20 ml of 10 mM Na oxalate pre-adjusted to pH 5.0 in order to introduce an environmentally realistic concentration of 100 μM oxalate into these suspensions.[8] The oxalate-amended Pb phosphate suspensions were then agitated on a rotary shaker for 24 hours. All suspensions, both with and without oxalate, were filtered using Whatman #42 filter papers to separate precipitates from the solution phases. The solutions were acidified with reagent-grade concentrated HNO_3 prior to analysis for total dissolved Pb and P by ICP-emission. Although Whatman #42 filter paper has a nominal pore size of 2.5 μm, we tested its efficiency in removing the microcrystalline Pb phosphate mineral particles formed at pH 6 and higher from the solution phase, and found it to be equally as effective as 0.2 μm nitrocellulose membrane filters used in some phases of the present work.

Pb phosphate precipitation in the presence of high oxalate concentration

This experiment tested the competitive effect of oxalate on Pb phosphate precipitation when the initial mole ratio of oxalate to phosphate was close to one. A 250 mM Na-oxalate stock solution was prepared in deionized water and subsequently pre-adjusted to pH 4.0 using concentrated nitric acid (HNO_3). Quantities of this solution and the previously described Na phosphate and $Pb(NO_3)_2$ stock solutions were used to prepare (in three replicates) 100-mL volumes of aqueous solutions of 10 mM

Pb^{2+} combined with 50 mM oxalate alone, or 50 mM oxalate and 66 mM phosphate. In order to prevent precipitation of Pb as an hydroxide or oxide mineral, the $Pb(NO_3)_2$ solution was always added as the last component after pre-adjustment of the phosphate and oxalate stock solutions to pH 5.0, 6.0, 7.0 and 8.0 using concentrated NaOH. The prepared solutions were then gently agitated at 22°C for 10 days, after which the pH was measured to determine the effect of chemical reactions in shifting the solution pH. Thereafter, the solution pH was re-adjusted to the initial target pH values (pH 4.0, 5.0, 6.0, 7.0, or 8.0). The solutions were subsequently equilibrated for 24 hours before filtration using Whatman #42 filter papers to separate precipitates from the solution phases. The filtrates were acidified with concentrated HNO_3 to a final concentration of 1.0 M HNO_3. Subsequently, the quantitation of Pb concentration was determined by flame atomic absorption (FAA) spectrophotometry and verified by ICP-AES using matrix-matched Pb standard solutions made up in 1.0 M HNO_3 from a certified Pb stock solution. Blank 1.0 M HNO_3 solutions and sample replicates were analyzed simultaneously to assure accuracy. The oxalate-containing systems had Pb solubilities within the range of quantitation for FAA, and a very good linear relationship ($r^2=0.997$) between measurements of dissolved Pb by FAA and ICP-AES. However, as the detection limit of FAA was higher than that of ICP-AES, about 0.1 mg L^{-1} for the most sensitive 217 nm absorption line, FAA was not sufficiently sensitive to measure dissolved Pb in the less soluble phosphate-only systems.

Kinetics of Mineral Precipitation and Transformation in the Pb phosphate-oxalate system at pH 5

The kinetics of Pb precipitation and potential for transformation between the initially precipitated Pb oxalate and Pb phosphates solid phases was followed at an initial pH of 5. As described above, solutions containing 10 mM Pb, 66 mM phosphate and 50 mM oxalate were prepared in duplicate from stock solutions pre-adjusted to pH 5.0. The resulting suspensions were agitated on a rotary shaker, and 15 ml subsamples of the suspensions were collected after 1 hr, 1 day, 5 days, 15 days and 30 days equilibration time. After the suspension pH values were measured, they were filtered through 0.2 µm nitrocellulose membranes and saved for ICP-AES analysis of dissolved Pb and P. The filtered solids were repeatedly washed in deionized water, then dried and analyzed by Fourier Transform Infrared (FTIR) spectroscopy and X-ray diffraction (XRD) to identify the predominant mineral phases.

FTIR and XRD Measurements

Prior to spectroscopic analysis, all Pb mineral precipitates collected on the filter papers and membranes as described above were repeatedly washed (3-4 times) with deionized water to remove soluble salts followed by air-drying. For comparative analysis, pure mineral precipitates of PbC_2O_4, $Pb_3(PO_4)_2$, and $PbHPO_4$ and hydroxypyromorphite $[Pb_5(PO_4)_3OH]$, prepared in accordance with previously published methods[11,12,22,23] were also analyzed by both FTIR and XRD.

The FTIR spectra of the mineral precipitates were collected using a Bruker Vertex 70 spectrometer (Bruker Optics Inc., Billerica, MA) equipped with a Pike GladiATR accessory (Pike Technologies, Madison, WI). Samples were analyzed using a single reflection diamond internal reflection element. Spectra were collected from 4500-150 cm^{-1} with a resolution of 2 cm^{-1}, with each spectrum representing an average of 100 co-added scans. Post-hoc smoothing (9-point Savitzky-Golay) and normalization were performed with OPUS 7.2 (Bruker Optics Inc.) software.

For XRD analysis, the mineral precipitates were water-washed, air-dried and ground with mortar and pestle prior to loading into a 0.2mm depth Anton Paar XRD sample holder. The XRD profiles were recorded with a Bruker D8 Advance powder X-ray diffractometer operated at 40 kV and 40 mA and equipped with an Anton Parr Eurotherm TCU110 temperature control unit and an Anton Paar CHC+ temperature and humidity chamber equipped with a Prolumid MHG-32 Modular Humidity Generator. Samples were equilibrated and maintained in the sample chamber at constant temperature (25 °C) and constant relative humidity (30%). The scanning parameters were 0.02° 2θ step size and 8 seconds as the counting time per step over the 10-43° 2θ Cu Kα angular range (λ = 1.54060 Å).

Results and Discussion

Pb solubility and precipitation in the phosphate-only systems

In all the prepared solutions of Pb with phosphate only, the formation of visible white precipitates indicated that the initial solution concentrations of Pb exceeded the solubility product of one or more Pb phosphate minerals over the entire experimental pH range. Figure 1 shows the Pb solubilities measured by ICP-AES in the pH range of 4.0 to 8.0 after 10 days and 7 months of aging. A minimum in Pb solubility near pH 6 was observed at both times, with the longer aging time reducing Pb solubility to a small degree, but only in the acidic pH range (4 to 6) (Figure 1). We also compared the measured Pb solubilities to those predicted by the widely used Pb phosphate mineral solubility products found in geochemical data compilations such as that of Lindsay[20] as well as databases of chemical speciation programs such as Visual MINTEQ (Figure 1)[17]. Over most of the pH range, measured Pb solubility was greater than expected from these generally accepted solubility products for the least soluble Pb phosphate minerals, $PbHPO_4$, $Pb_5(PO_4)_3OH$ and $Pb_3(PO_4)_2$ (see Equations 1-3) (Figure 1).

The discrepancy between our experimental data and model estimates was relatively minor at pH 4.0 where our data were in close agreement with the predicted soluble Pb in equilibrium with the formation of $PbHPO_4$ (Figure 1). However, disagreement between our data and the modeling results became increasingly significant in the pH range of 5.0 to 8.0. Previous studies have also presented evidence that some Pb-phosphate minerals have a lower formation constant (i.e., higher solubility) than commonly assumed. For instance, the formation constant for $Pb_5(PO_4)_3Cl$ was reported to be up to 5 log units lower than the widely used value in previous publications and chemical speciation programs.[12,18,19]

We attribute previous underestimation of the solubility of Pb-phosphate minerals, which was pronounced in the pH range of 6.0 to 8.0, to the earlier assumption that the solubility product determined at pH less than 3 would be also applicable at much higher pH[16], a potentially large source of error discussed by Xie and Giammar.[18] Another notable difficulty in determining accurate solubility product relationships and saturation indices for Pb-phosphate systems in earlier work was the fact that total dissolved Pb rather than free Pb^{2+} activity in solution was measured, so that soluble Pb^{2+} ion pairs with phosphate, hydroxide, and bicarbonate could have affected the estimates of ion activity products in solution.[10] Here, we addressed this problem by estimating Pb^{2+} activity directly in the Pb-phosphate systems after 7 months aging time using the Pb ion-selective electrode. The measured and calculated (by Visual MINTEQ) Pb^{2+} ion activities as a function of pH were compared to Pb solubility (Figure 2). The electrode-measured Pb^{2+} activities were greater than the predicted values and this discrepancy became most pronounced at pH greater than 6.0. In addition, in the same pH range, the much higher dissolved Pb concentration compared to free Pb^{2+} indicated that most of the soluble Pb was complexed (Figure 2), most likely with phosphate anions.

Speciation programs calculate the free Pb^{2+} activity after estimating the fraction of dissolved Pb expected to be in soluble complexes with anions such as phosphate, bicarbonate, and hydroxide.[24] However, to the best of our knowledge, there are no reliable measurements of the stability constants of dissolved $PbHPO_4^0$ and $PbH_2PO_4^+$ ion pairs; these constants have been instead estimated in the databases of chemical equilibrium programs using analogy with measured stabilities of other metal-phosphate ion pairs.[25] Based on our results here with Pb in solutions containing high dissolved phosphate, we suggest that soluble $PbH_2PO_4^+$ and particularly $PbHPO_4^0$ ion pairs have been underestimated in chemical speciation programs and may account for the much greater measured solubility of Pb relative to the free Pb^{2+} concentration at pH higher than 6.0 (Figure 2). In natural soil or water systems, phosphate concentrations would be much lower than those in the aqueous solutions studied here, and Pb-phosphate ion pairs would likely be minor species compared to complexes with OH^-, bicarbonate and organic acids. Pan and Darvell[26] have concluded that a major contributor to the poor agreement among various estimates of solubility products for phosphate minerals of the apatite type is the inability to estimate correctly concentrations of the various metal ion pairs in solution. In addition, these phosphate mineral structures tend to dissolve incongruently due to the exchange of surface metal ions (Ca^{2+}, Pb^{2+}) into solution with H^+ ions.[23] As a result, measured ion activity products of solutions in equilibrium with Pb phosphates are often not in accordance with the mineral phases actually present[10] and the assumption of invariant solubility products for minerals such as apatite and hydroxypyromorphite may be invalid[26].

Pb phosphate precipitation in the presence of high and low oxalate concentrations

The introduction of high concentrations of oxalate into the Pb-phosphate systems, at concentrations approximately equimolar with phosphate, inhibited Pb precipitation and thus caused Pb solubility to be greatly increased at all pH values below 7 (Figure 3A). Compared to the solutions with phosphate alone, dissolved Pb was 30 to 200 times greater with both oxalate and phosphate present in solutions (Figure 3A). Experiments conducted with oxalate alone showed that a high Pb solubility was maintained ($10^{-4.5}$ M) over the entire pH range tested (Figure 3A). The high Pb solubility with oxalate alone can be attributed to the formation of stable and soluble $Pb(C_2O_4)^0$ and $Pb(C_2O_4)_2^{2-}$ complexes, both of which were predicted using the Visual MINTEQ modeling program to comprise nearly all of the dissolved Pb. However, the measured Pb solubilities in the Pb-oxalate and Pb-phosphate-oxalate system ($10^{-4.5}$ M) were significantly lower than predicted ($10^{-3.2}$

M) by Visual MINTEQ. We posit that a lower solubility product of PbC_2O_4 than previously assumed may be responsible for the discrepancy between measured and predicted Pb solubilities for the oxalate-containing systems with or without phosphate. Thus, chemical model predictions underestimated the extent to which oxalate would compete with phosphate for Pb precipitation and complexation, especially at lower pH. The log formation constant for PbC_2O_4 precipitation was more recently determined to be 11.13, substantially greater than the older log K estimate of 8.94 used in numerous chemical equilibrium models.[22] Furthermore, the log formation constants for the dissolved 1:1 and 1:2 Pb-oxalate complexes were determined to be 5.85 and 8.05, respectively, greater than the corresponding values of 5.12 and 7.13 used in the Visual MINTEQ database.[22] Nevertheless, the Visual MINTEQ program using either the older or more recent estimates of these formation constants qualitatively predicted the observed pH-dependent effect of oxalate in modifying Pb phosphate mineral stability.

The solubility data for the mixed Pb-phosphate-oxalate system indicated that, at pH 5.0 and lower, Pb solubility was controlled by Pb oxalate precipitation (Figure 3A). However, at pH 7.0 and above, Pb solubility was limited by the precipitation of Pb phosphates despite the presence of oxalate. At the intermediate pH of 6.0, our data indicated that the presence of oxalate still partially suppressed the control of Pb solubility by phosphate, causing Pb to be more soluble than in the presence of phosphate alone (Figure 3A). As shown in Equations 1-4, the release of H^+ from the formation of Pb-phosphate minerals is expected to decrease the solution pH whereas the formation of PbC_2O_4 represents a 1:1 complexation reaction with the $C_2O_4{}^{2-}$ anion resulting in minimal pH change, except possibly at the lowest pH of 4 where oxalic acid is partially protonated. Accordingly, for the systems that contained Pb with phosphate alone, we recorded a pH change of about -1.5 to -2.0 when the initial pH was less than 6.0 and about -0.25 to -0.6 at initial pH of 6.0 and greater (Figure 3B). By contrast, the oxalate-only systems showed a relatively small pH change, from about

+0.1 to -0.4, throughout the entire experimental pH range tested (Figure 3B). For the solutions containing both oxalate and phosphate, the pH decreased to a similar extent as those of the phosphate-only systems at pH 6 and higher, implying a similar degree of Pb-phosphate mineral formation (Figure 3B). However, at solution pH less than 6.0, the large pH decreases observed for the phosphate-only systems were largely eliminated when oxalate was present with phosphate (Figure 3B). Therefore, change in the solution pH upon mineral precipitation provided indirect evidence for the inhibition of Pb-phosphate precipitation by oxalate at pH less than 6.0 (Figure 3B). Both FTIR and XRD analysis of the mineral phases formed, as discussed in the next two sections, further confirmed the solubility data regarding which anionic ligand (i.e, phosphate or oxalate) controlled the precipitation reactions.

The high concentrations of oxalate present in the systems described above were able to compete with phosphate for complexation and precipitation of Pb, particularly in the acidic pH range. In order to test whether low oxalate concentrations could solubilize Pb phosphates previously precipitated, we equilibrated Pb phosphate minerals formed at pH 4.0, 6.0, and 8.0 with 100 µM oxalate in pH 5.0 Na-acetate buffer; the Pb phosphate minerals were pre-washed to remove excess salts prior to exposure to oxalate. The measured Pb solubilities indicated a small amount of dissolution of Pb by oxalate (Figure 4) whereby $PbHPO_4$, which was formed at pH 4.0, was the most susceptible to oxalate-induced dissolution compared to the Pb phosphates formed at higher pH. Dissolved phosphate in these buffered pH 5 systems ranged from about 0.7 mM from the pH 4 minerals to less than 0.1 mM for the pH 8 minerals (Figure 4). However, dissolved phosphate concentrations increased upon oxalate addition to the pH 6 and 8 Pb phosphates. These results point to the stability of Pb phosphates under mildly acidic conditions in the presence of acetate and oxalate at low concentrations, but also indicate that biologically produced oxalate could raise Pb solubility in soils containing Pb phosphates.

FTIR Analysis of Mineral Precipitates

We employed FTIR spectroscopy to identify qualitatively the mineral composition with respect to Pb oxalate and/or Pb phosphate precipitation in the phosphate-oxalate mixed systems. For comparative analysis, we also obtained FTIR spectra of Pb precipitates formed from reactions with only phosphate or only oxalate (Figure 5). The spectral features in the oxalate-only systems prepared at all the pH values (pH 4.0 to 8.0) showed the diagnostic vibrations characteristic of PbC_2O_4 anhydrate: ν_{as} COO- at 1564 cm^{-1}, ν_s COO- and ν C-C at 1363 cm^{-1}, δ O-C-O and ν Pb-O at 770 cm^{-1}, δ O-C-O at 501 cm^{-1}, and δ O-C-O and ν C-C at 371 cm^{-1}, respectively.[27-29] With respect to the FTIR spectra of the phosphate-only precipitates, distinct forms of Pb-phosphate minerals were identified depending on the aqueous pH conditions (Figure 5). At pH 4.0 and 5.0, the FTIR spectra of the precipitates from phosphate-only were indicative of the formation of $PbHPO_4$ with the following characteristic vibrations: ν_1 O-P-O at 912 cm^{-1}, ν_3 O-P-O at 980 cm^{-1}, ν_4 O-P-O at 542 cm^{-1} and 367 cm^{-1}.[30,31] However, at higher pH values (pH 6.0-8.0), the spectral peaks of the precipitated solids from the phosphate-only solutions closely matched those of synthetic $Pb_3(PO_4)_2$ with the following prevalent peaks: ν_3 asymmetric O-P-O stretch at 1017 (shoulder), 979 (shoulder) and 955 cm^{-1}; ν_4, O-P-O bend at 579, 550 and 533 cm^{-1}; and, weaker ν_2 phosphate bending vibrations at 447, 425 cm^{-1}, and 384 cm^{-1} (Figure 5). Although the 384 cm^{-1} vibration is absent from the FTIR spectrum of $Pb_5(PO_4)_3OH$ and clearly present in the spectrum of $Pb_3(PO_4)_2$, we cannot rule out the possibility that both $Pb_3(PO_4)_2$ and $Pb_5(PO_4)_3OH$ were precipitating in the phosphate-only solution from pH 6.0 to pH 8.0 (Figure 5).

The FTIR spectra of the minerals precipitated from the mixed Pb oxalate-phosphate solutions revealed that the solution pH condition controlled whether Pb precipitated with oxalate or with phosphate (Figure 5). At the lower pH range (4.0 and 5.0), the FTIR spectra were nearly identical to the spectra of the precipitates from the oxalate-only solutions (Figure 5). There was no FTIR evidence of the presence of Pb-phosphate minerals in the precipitates formed under these acidic conditions. Therefore, the precipitation of PbC_2O_4 superseded the precipitation of $PbHPO_4$ at pH 4.0 and 5.0 (Figure 5). At the higher pH range (6.0 to 8.0), the FTIR spectra of the precipitates from the mixed-ligand solutions all closely matched the spectra of the precipitates from the phosphate-only solutions over the same pH range wherein the peaks implied the presence of $Pb_3(PO_4)_2$ or both $Pb_3(PO_4)_2$ and $Pb_5(PO_4)_3OH$(Figure 5). Some weak FTIR features attributable to a PbC_2O_4 precipitate were present at pH 6.0 but not at higher pH (Figure 5).

As all of the FTIR results described above were obtained at an equilibration time of 10 days, additional experiments were conducted to determine whether kinetics may have favored the precipitation of Pb oxalate relative to Pb phosphate. The precipitation reaction was followed over the interval of 1 hour to 30 days at pH 5.0, a pH at which the 10-day equilibration had shown Pb oxalate formation to be favored over Pb phosphate. Over the longer reaction time of 30 days, we observed a slow increase in pH, some increase in Pb solubility from 30 μM to 50 μM, and a decrease in dissolved phosphate (Figure 6A). We also found that the FTIR spectra of the precipitated solids changed over this time period. Consistent with the FTIR spectrum observed at 10 days, Pb-oxalate was the predominant solid formed initially (1 hr); after 30 days, however, the FTIR spectrum of the precipitate showed diagnostic features of both Pb phosphate and Pb oxalate (Figure 6B). These temporal data of both solution and precipitate analyses implied partial decomposition of oxalate with consumption of protons as follows:

$$H^+{}_{(aq)} + C_2O_4{}^{2-}{}_{(aq)} = CO_2 + HCOO^- \qquad (5)$$

The partial transformation of Pb oxalate to Pb phosphate, revealed by FTIR spectroscopy, could not in itself explain the increase in pH observed over time (Figure 6A). However, oxalate decomposition would raise pH while releasing Pb from previously precipitated oxalate to form Pb phosphate. Therefore, the most likely explanation for the effect of the extended reaction time on the composition of the mineral precipitates formed is microbial decomposition of a fraction of the oxalate in the non-sterile solutions.

XRD Identification of Mineral Precipitates

We performed XRD analysis to identify the mineral structures and estimate semi-quantitatively the relative concentrations of crystalline Pb phosphate and oxalate minerals formed in the solid precipitates at the 10-day reaction time (Figure 7). First, as reference XRD patterns, we obtained diffractograms of pure mineral precipitates of PbC_2O_4 and the three Pb-phosphates that are known to form under the experimental conditions investigated (Figure 7A). The major XRD peaks of PbC_2O_4 were at 18.54, 18.7, 21.14, 23.56, and 27.3 degrees 2θ, similar to data in previous studies.[6,32] The XRD pattern of synthetic $PbHPO_4$ demonstrated major peaks at 13.36 and 26.86 degrees 2θ, which matched well with a previous result[30] (Figure 7A). The XRD pattern of $Pb_5(PO_4)_3OH$was distinguished by its peaks at 20.9, 21.7, 26.3, 27.7, 30.2 and 31.5 degrees 2θ (Figure 7A).[33,34] [4]

Over the entire experimental pH range (pH 4.0 to 8.0), the XRD patterns of the precipitates from the oxalate-only solution had major peaks at 18.6, 19.6, 20.8, 21.2, 23.7, 26.3, and 27.1 degrees 2θ, which were in close agreement with pure PbC_2O_4 (Figures 7A and 7B). However, the mineral precipitates from the phosphate-only solutions exhibited pH-dependent XRD patterns (Figure 7A). At pH 4.0 and pH 5.0, the diffractograms had defined peaks at 13.4, and 26.8 degrees 2θ, which were characteristic of pure $PbHPO_4$ (Figure 7B). By contrast, at the three highest experimental pH values (pH 6.0, 7.0 and 8.0) in the phosphate-only system, the characteristic peaks of the diffractograms at 21.0, 22.0, 26.9, 27.9, 30.6, and 31.8 degrees 2θ were consistent with both $Pb_3(PO_4)_2$ and/or $Pb_5(PO_4)_3OH$ (Figure 7C).

In the presence of both oxalate and phosphate, the XRD mineral identifications supported the FTIR results, indicating that the formation of PbC_2O_4 was preferred over that of $PbHPO_4$ at pH 4.0 and 5.0 (Figure 7B). Similar to the data obtained for the phosphate-only system, at higher pH values (pH 6.0 to 8.0) the XRD data is again consistent with the presence of both $Pb_3(PO_4)_2$ and $Pb_5(PO_4)_3OH$ (Figure 7C).

Conclusions

The results of this study provide insights on how soil environments enriched in oxalate or related low-molecular-weight compounds could interfere with the sequestration of Pb into insoluble Pb phosphate minerals. Our findings imply that, at equimolar concentrations of oxalate and phosphate, Pb-phosphate minerals would be insufficiently stable to control Pb solubility in acidic environments, but would be able to form or persist in the presence of oxalate at pH 6 and higher. Although we have focused on conducting most of our experiments at a specific oxalate:phosphate ratio that is environmentally reasonable, the absolute concentrations used exceed those found in natural waters or soils. In our experiment with a targeted low oxalate concentration that might be expected in soils, oxalate forms sufficiently stable chelates with Pb to raise the solubility of Pb in equilibrium with Pb-phosphate minerals. Our measurements of Pb solubilities and free Pb^{2+} ion activities in aqueous solutions containing oxalate and phosphate indicate that solubility products for Pb-oxalate and Pb-phosphate minerals and Pb-phosphate ion pairing constants used widely in chemical equilibrium models are in need of correction. Specifically, the reported solubility products of the Pb-phosphate minerals formed at pH 6 and higher [$Pb_5(PO_4)_3OH$ and $Pb_3(PO_4)_2$] predict much lower Pb solubilities than observed in our experiments.

Author Information

Corresponding Author

*e-mail: mbm7@cornell.edu (Murray B. McBride)

ORCID

Michael P. Schmidt: 0000-0001-8789-9204

Carmen Enid Martínez: 0000-0001-8553-2118

Sonam Sherpa : 0000-0003-1758-3399

Ludmilla Aristilde: 0000-0002-8566-1486

Murray McBride : 0000-0003-0915-6688

Notes

The authors declare no competing financial interest.

Acknowledgement

We are grateful to Xiaoyan Tang for her technical assistance in the laboratory.

We acknowledge research funding from the National Institute of Food and Agriculture (Hatch project NYC-125400) awarded to M.B.M. and graduate student support for S.E.K. and M.P.S. provided by an Integrative Graduate Education and Research Traineeship (IGERT) research fellowships from the National Science Foundation.

References

1. M. Cai M, M.B. McBride and K. Li, Bioaccessibility of Ba, Cu, Pb and Zn in urban garden and orchard soils. *Environ. Pollut.*, 2016, **208**,145-152.

2. N.R. Atkinson, E.H. Bailey, A.M. Tye, N. Breward and S.D. Young, Fractionation of lead in soil by isotopic dilution and sequential extraction*. Environ. Chem.*,2011, **8**, 493-500.

3. L. Mao, E.H. Bailey, J. Chester, J. Dean, E.L. Ander, S.R. Chenery and S.D. Young, Lability of Pb in soil: effects of soil properties and contaminant source. *Environ. Chem.,*2014*,* **11**, 690-701.

4. E.R. Marzouk, S.R. Chenery and S.D. Young, Measuring reactive metal in soil: a comparison of multi-element isotopic dilution and chemical extraction. *J. Soil Science*, 2013, **64**, 526-536.

5. H. Henry, M.F. Naujokas, C. Attanayake, N.T. Basta, Z. Cheng, G.M. Hettiarachchi, M. Maddaloni, C. Schadt and K.G. Scheckel, Bioavailability-based in situ remediation to meet future lead (Pb) standards in urban soils and gardens. *Environ. Sci. Technol*., 2015, **49**, 8948-8958.

6. J.A. Sayer, J.D. Cotter-Howells, C. Watson, S. Hillier and G.M. Gadd, Lead mineral transformation by fungi*. Curr. Biol.*, 1999, **9**, 691-694.

7. N.S. Bolan, R. Naidu, S. Mahimairaja and S. Baskaran, Influence of low-molecular-weight organic acids on the solubilization of phosphates. *Biol. Fert. Soils*,1994,**18**, 311-319.

8. D.L. Jones, Organic acids in the rhizosphere- a critical review. *Plant Soil*, 1998, **205**, 25-44.

9. W. Wei, Y. Wang, Z. Wang, R. Han, S. Li, Z. Wei and Y. Zhang, Stability of chloropyromorphite in ryegrass rhizosphere as affected by root-secreted low molecular weight organic acids. *PLoS ONE* , 2016, **11**: e0160628.doi:10.1371.

10. S. Sauvé, M. McBride and W. Hendershot, Lead phosphate solubility in water and soil suspensions. *Environ. Sci. Technol*. , 1998, **32**, 388-393.

11. F. Lang and M. Kaupenjohann, Effect of dissolved organic matter on the precipitation and mobility of the lead compound chloropyromorphite in solution. *Eur. J. Soil Sci.*, 2003, **54**, 139-147.

12. C.E. Martinez, A.R. Jacobson and M.B. McBride, Lead phosphate minerals: Solubility and dissolution by model and natural ligands. *Environ. Sci. Technol.*, 2004, **38**, 5584-5590.

13. F. Debela, J.M. Arocena, R.W. Thring and T. Whitcombe, Organic acid-induced release of lead from pyromorphite and its relevance to reclamation of Pb-contaminated soils. *Chemosphere* , 2010, **80**, 450-456.

14. F. Debela, J.M. Arocena, R.W. Thring and T. Whitcombe, Organic acids inhibit the formation of pyromorphite and Zn-phosphate in phosphorus amended Pb- and Zn-contaminated soil. *J. Environ. Manage.*, 2013, **116**, 156-162.

15. J.O. Nriagu, Lead orthophosphate. I. Solubility and hydrolysis of secondary lead orthophosphate. *Inorg. Chem.*, 1972, **11**, 2499-2503.

16. J.O. Nriagu, Lead orthophosphates-II. Stability of chloropyromorphite at 25 °C. *Geochim. Cosmochim. Acta*, 1973, **37**, 367-377.

17. Gustafsson J.P. (2018) Visual MINTEQ 3.1, http://www.lwr.kth.se/english/OurSoftWare/Vminteq/index.html

18. L. Xie and D.E. Giammar, Equilibrium solubility and dissolution rate of the lead phosphate chloropyromorphite. *Environ. Sci. Technol.*, 2007, **41***,* 8050-8055.

19. J. Flis, M. Manecki and T. Bajda, Solubility of pyromorphite $Pb_5(PO_4)_3Cl$- mimetite $Pb_5(AsO_4)_3Cl$ solid solution series. *Geochim. Cosmochim. Acta*, 2011, **75**, 1858-1868.

20. W.L. Lindsay. 1979. Chemical Equilibria in Soils. J. Wiley and Sons, New York.

21. K.G. Scheckel and J.A. Ryan, Effects of aging and pH on dissolution kinetics and stability of chloropyromorphite. *Environ. Sci. Technol.*, 2002, **36***,* 2198-2204.

22. Y. Xiong, L. Kirkes, T. Westfall and R. Roselle, Experimental determination of solubilities of lead oxalate (PbC_2O_4(cr)) in a NaCl medium to high ionic strengths, and the importance of lead oxalate in low temperature environments. *Chem. Geol.*, 2013, **342**, 128-137.23. Y. Zhu, Z. Zhu, X. Zhao, Y. Liang, Y. Huang, Characterization, dissolution and solubility of lead hydroxypyromorphite [$Pb_5(PO_4)_3OH$] at 25-45^{o}C. *J. Chem.,2015,* doi.org/10.1155/269387.

24. S. Sauvé, M.B. McBride and W.H. Hendershot, Speciation of lead in contaminated soils. *Environ. Pollut.*, 1997, **98**, 149- 155.

25. C.W. Childs, A potentiometric study of equilibria in aqueous divalent metal orthophosphate solutions. *Inorg. Chem.*,1970, **9**, 2465-2469.

26. H.B. Pan, B.W. Darvell, Calcium phosphate solubility: the need for re-evaluation. *Crystal Growth & Design,* 2009, **9**, 639-645.

27. J. Fujita, A.E. Martell and K. Nakamoto, Infrared spectra of metal chelate compounds. VI. A normal coordinate treatment of oxalate metal complexes. *J. Chem. Phys.,*1962, **36***,* 324-331.

28. R.L. Frost, Y. Jing and Z. Ding, Raman and FTIR spectroscopy of natural oxalates: Implications for the evidence of life on Mars. *Chinese Sci. Bull.*, 2003, **48***,* 1844-1852.

29. N. Mancilla, M.C. D'Antonio, A.C. González-Baró and E.J. Baramn, Vibrational spectra of lead(II) oxalate. *J. Raman Spectr*osc., 2009, **40**, 2050-2052.

30. O. Saisa-ard and K.J. Haller, Crystallization of lead phosphate in gel systems. *Eng. J.*, 2012, **16**, 161-168.

31. Y. Zhu, B. Huang, Z. Zhu, H. Liu, Y. Huang, X. Zhao and M. Liang, Characterization, dissolution, and solubility of the hydroxypyromorphite solid solution $(Pb_xCa_{1-x})_5(PO_4)_3OH$ at 25^{o}C and pH 2-9. *Geochem. Trans.*, 2016, **17**: 2.

32. M.M. Khunur, D.T. Wahyuni and Y.P. Prananto, Synthesis of lead(II) oxalate hydrate ($PbC_2O_4 \cdot xH_2O$) crystal In silica gel. *Adv. Nat. Applied Sci.*, 2011, **5,** 467-472.

33. P. Zhang and J.A. Ryan, Formation of pyromorphite in anglesite-hydroxyapatite suspensions under varying pH conditions*. Environ. Sci. Technol.*, 1998, **32**, 3318-3324.

34. J.D. Hopwood, G.R. Derrick, D.R. Brown, C.D. Newman, J. Haley, R. Kersaw and M. Collinge, The identification and synthesis of lead apatite minerals formed in lead water pipes*. J. Chem.*, 2016, DOI:10.1155/9074062.

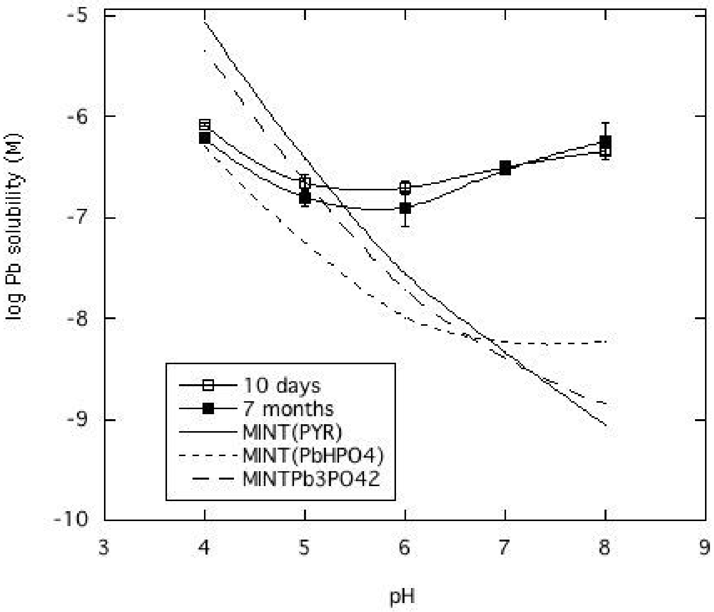

Figure 1: Measured (by ICP-AES) and predicted total dissolved Pb concentrations as a function of pH in aqueous solutions initially containing 10 mM Pb and 66 mM phosphate, aged for 10 days and 7 months. Predicted solubility lines for hydroxypyromorphite (PYR), $PbHPO_4$ and $Pb_3(PO4)_2$ using Visual MINTEQ (MINT) are shown. Data values (average ± standard deviation) are from two independent replicates.

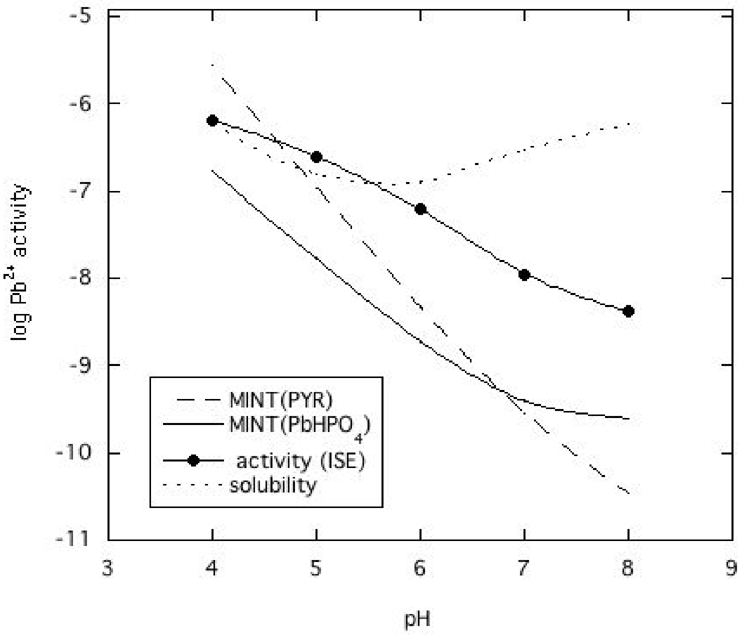

Figure 2: Measured (by ion-selective electrode) and predicted free Pb^{2+} ion activity as a function of pH in aqueous solutions initially containing 10 mM Pb and 66 mM phosphate, aged for 7 months. The corresponding total dissolved Pb (solubility) is plotted using a dotted line. Predicted Pb activities for hydroxypyromorphite (PYR) and $PbHPO_4$ using Visual MINTEQ (MINT) are shown for comparison. Data values (average ± standard deviation) are from two independent replicates.

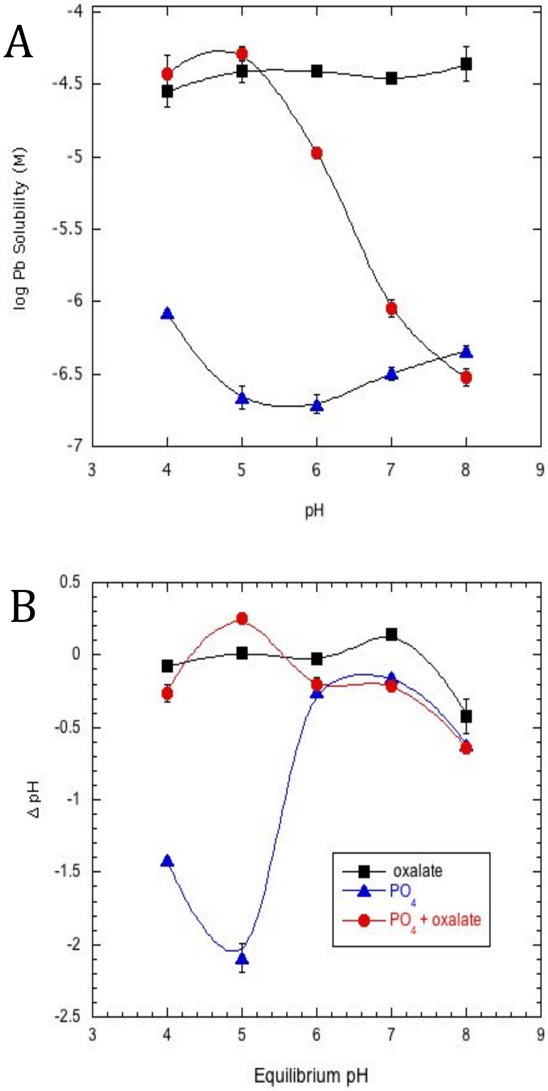

Figure 3: (A) Total dissolved Pb concentration as function of pH after 10 days reaction time in the presence of oxalate alone, phosphate alone, or both oxalate and phosphate; initial concentrations were 10 mM Pb, 66 mM phosphate and 50 mM oxalate. (B) Change between initial reaction pH and equilibrium reaction pH during Pb reactions with oxalate alone, phosphate alone, or both oxalate and phosphate. In A and B, data values (average ± standard deviation) are from two independent replicates.

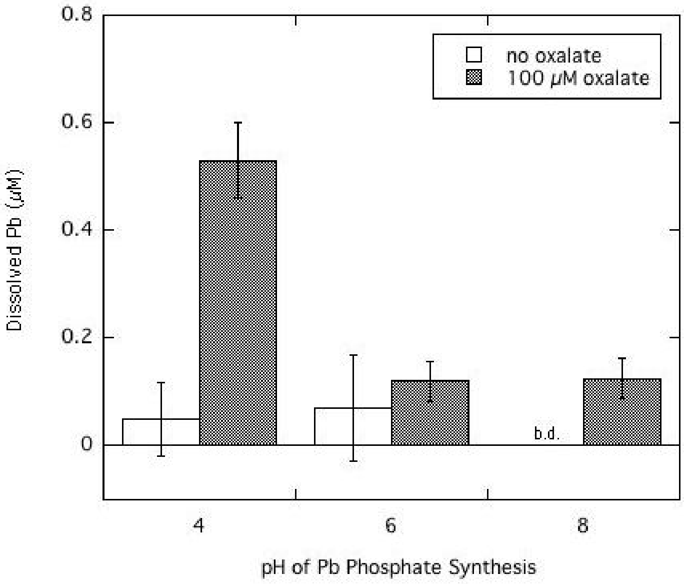

Figure 4: Effect of 100 µM oxalate on the solubility of Pb in equilibrium with Pb phosphate minerals precipitated at pH 4.0, 6.0, and 8.0. Total dissolved Pb concentrations are shown in the absence (white bars) and presence (grey bars) of oxalate.

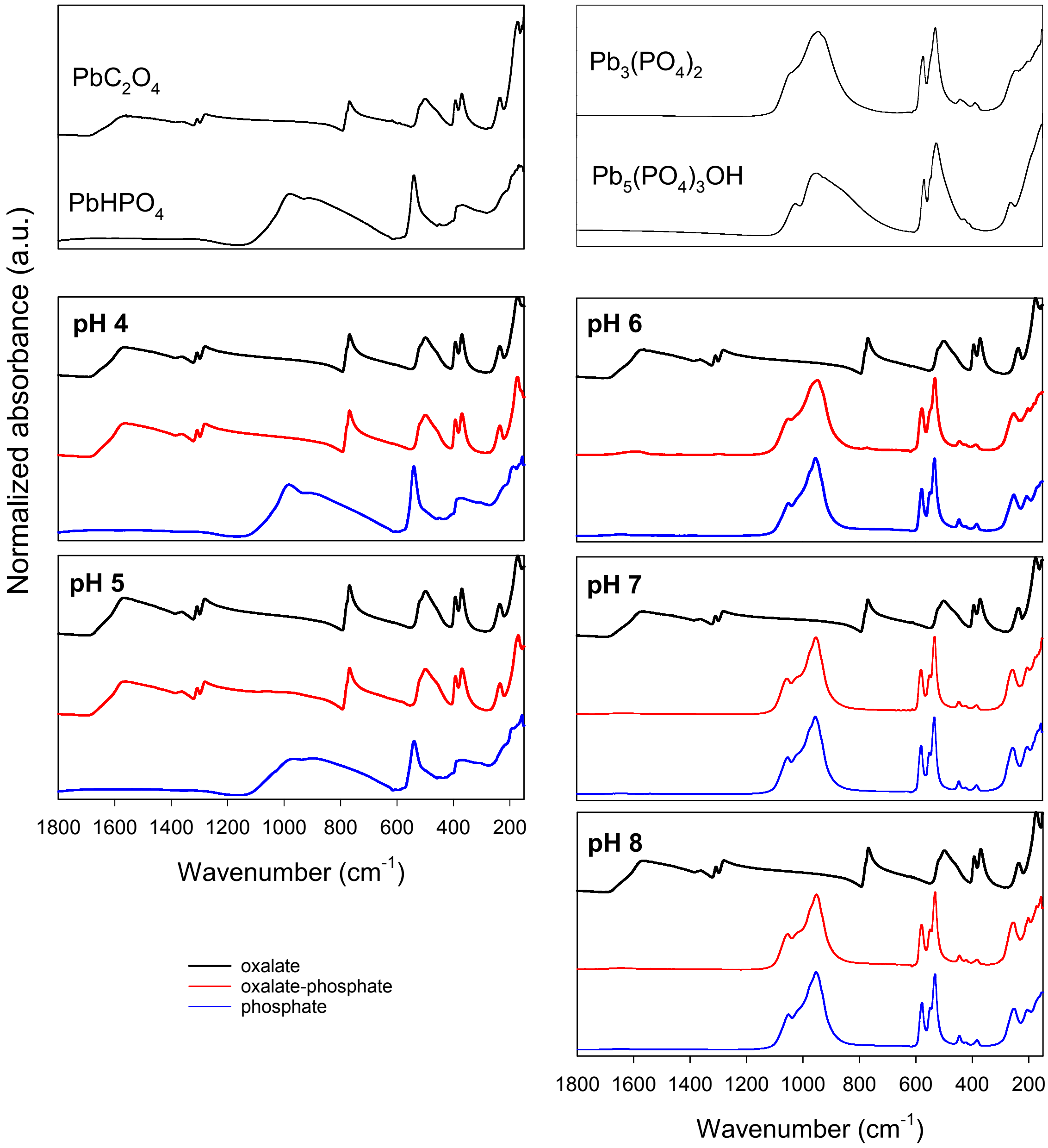

Figure 5. FTIR spectra of mineral standards (top panels) and precipitates collected at our studied pH values (as indicated within each panel) from experiments with Pb-oxalate (black, top spectra), Pb-oxalate/phosphate (red, middle spectra) and Pb-phosphate (blue, bottom spectra).

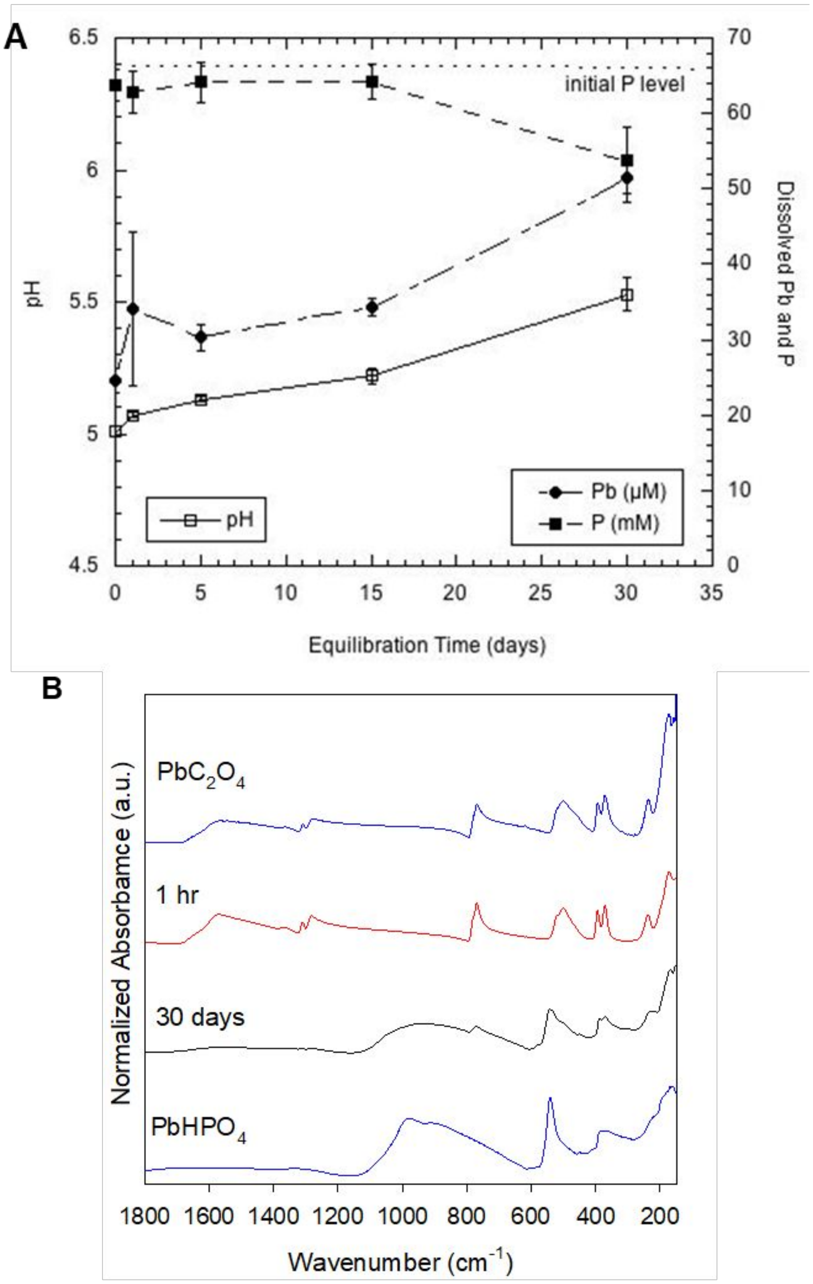

Figure 6: (A) Effect of reaction time on pH, total dissolved Pb and phosphate concentrations in the Pb-phosphate-oxalate mixed systems prepared at initial pH of 5. (B) FTIR spectra of Pb-oxalate/phosphate precipitates formed in the system described in (A) after 1 hour (red line) and 30 days (black line). The FTIR spectra (in blue) of pure Pb-oxalate and $PbHPO_4$ mineral phases are shown for comparison.

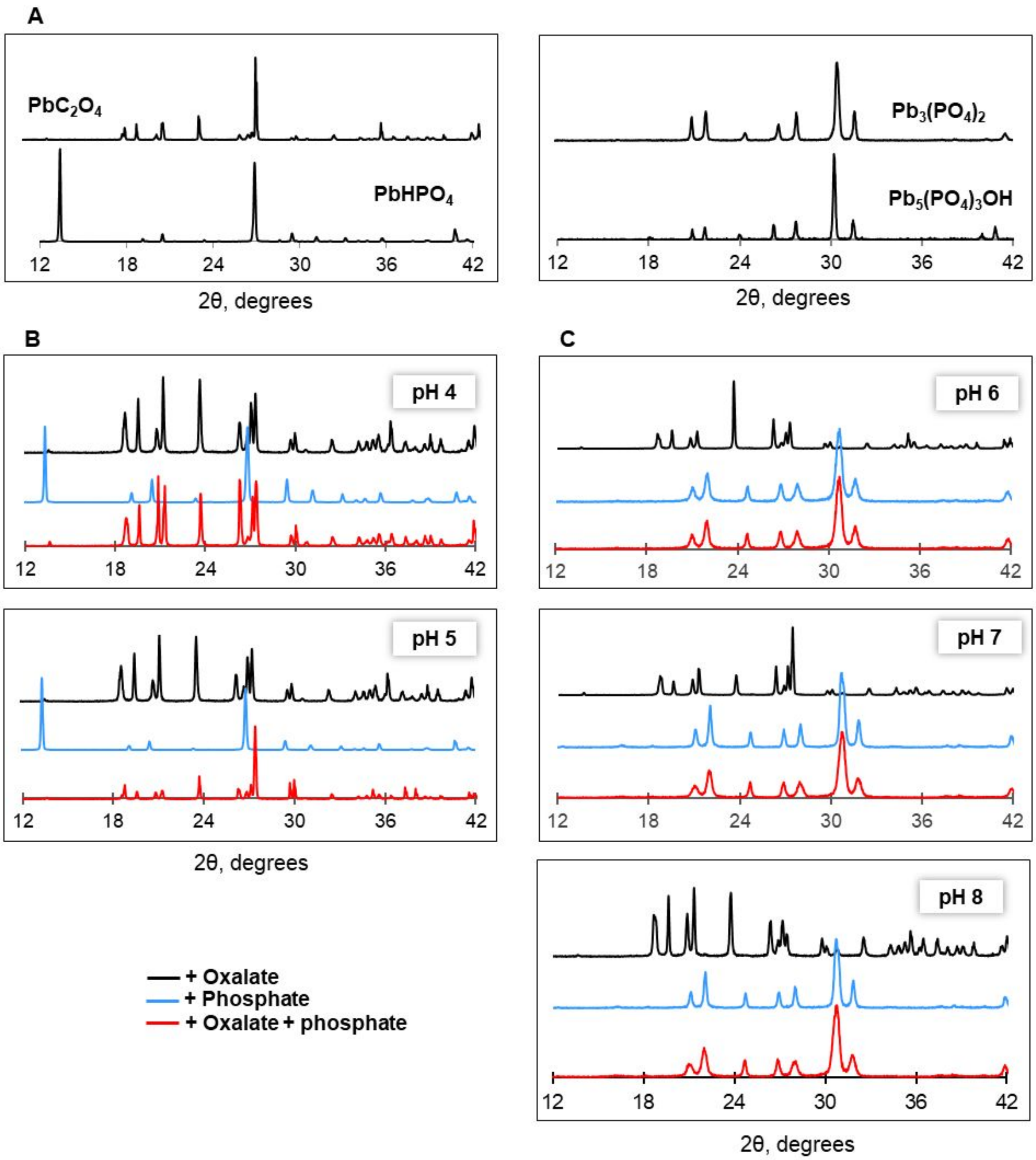

Figure 7. (A) XRD patterns of pure mineral precipitates prepared at pH 7.0. XRD patterns of mineral precipitates formed in solution at (B) pH 4.0 and pH 5.0, and at (C) pH 6.0, pH 7.0, and 8.0: oxalate alone (black), phosphate alone (blue), or both oxalate and phosphate (red).